Engineering Structures 215 (2020) 110443

Contents lists available at ScienceDirect

Engineering Structures

journal homepage: www.elsevier.com/locate/engstruct

Behaviour of circular SMA-confined reinforced concrete columns subjected to eccentric loading

Raafat El-Hacha[1], Khaled Abdelrahman*

Department of Civil Engineering, University of Calgary, Calgary, Alberta, Canada

ARTICLE INFO

Keywords:
Circular, confinement
Carbon
Ductility
Fibre reinforced polymer
Shape memory alloys
Strength

ABSTRACT

Shape Memory Alloys (SMA) are recently utilized for strengthening/repair of concrete structures. Commonly used SMA wires used for concrete confinement applications are those in Nickel-Titanium (*NiTi*), because they possess unique thermo-mechanical properties such as shape memory effect (SME) along with high recovery stress (up to 600 MPa) and strain (up to 8%). Initial investigations reported in the literature show actively confining concrete columns with SMA wires can enhance the strength and the ductility of concrete. To date, vast majority of experiments on SMA-confined concrete have considered short, unreinforced, small-scale concrete cylinders subjected to concentric axial loading. The objective of this study is to present a systematic study of circular SMA-confined reinforced concrete (RC) columns subjected to eccentric loading. Test data are compared against identical unconfined RC columns, and RC columns confined passively using conventional CFRP sheets. The results of this study show the RC columns confined with active SMA spirals exhibited significant enhancement in strength and ductility compared to unconfined RC columns subjected to varying load eccentricity. Additionally, the SMA-confined RC columns demonstrated superior overall performance when compared to the conventional passive CFRP-confined RC columns.

1. Introduction

Recent catastrophic failures due to earthquakes revealed the vulnerability of our infrastructure as investigations conducted on these structures showed the main cause of failure was associated with the collapse of concrete columns leading to progressive failure of the structure [1]. Repair and strengthening strategies of concrete columns are crucial to ensure the safety of the public and revive our current infrastructure to become structurally reliable to withstand future earthquake events.

One of the strengthening and repair strategies commonly adopted to enhance the performance of concrete columns is through confinement methods. Traditional confinement methods such as concrete casing and steel jacketing are considered ineffective, as the strengthening material suffers from the same deterioration effect as the parent material. On the other hand, the use of non-corrosive and light-weight materials such as Fibre-Reinforced Polymers (FRP) confines the concrete column by a passive confinement mechanism and only activates after significant damage is encountered in the concrete. Results from the limited research conducted to investigate the feasibility of actively confining FRP columns reported this confinement method was unpractical, expensive, and required excessive labour time [2–4]. Thus, there is a critical need to develop smart and innovative strengthening strategies for concrete columns.

Recently, a new class of smart materials termed Shape Memory Alloys (SMA) was introduced as a strengthening material to enhance the structural performance of concrete columns. The SMA's possess unique thermo-mechanical properties and material characterization which overcome the shortcomings of the above-mentioned confinement methods. The SMA's are commonly referred to as smart materials for their ability to sustain large deformations (up to 8%) and return to their original shape upon heating or unloading [5]. These unique properties of the SMA occur due to phase transformation of the material between the austenite phase and the martensite phase. The austenite and the martensite phases are related to the high temperature state and the low temperature state of the material, respectively. Recovering the original shape of the SMA after being deformed beyond its elastic limits through unloading is referred to as super-elasticity, and through heating is referred to as the Shape Memory Effect (SME). The SMA used in the form of wires, when wrapped around the column, can actively confine the concrete by utilizing its unique thermo-mechanical properties. Further information about the material characterization of the SMA can be

* Corresponding author. Tel.: 403-472-7403.
E-mail addresses: relhacha@ucalgary.ca (R. El-Hacha), kabdelra@ucalgary.ca (K. Abdelrahman).
[1] Tel.: 403-220-4817.

https://doi.org/10.1016/j.engstruct.2020.110443
Received 10 November 2019; Received in revised form 23 February 2020; Accepted 26 February 2020

found in Abdelrahman and El-Hacha [6].

2. Research significance

The potential advantage realized through the very limited research conducted on SMA-confined concrete columns create opportunities for further areas of research to be investigated. To date, the research focus has been to characterize the behaviour of SMA-confined concrete columns subjected to concentric and cyclic loading conditions [7–9]. Equally important is understanding the effects of eccentric loading on SMA-confined concrete columns. Despite its importance, there are no research studies found in the literature that address this subject. Thus, the objective of this study is to investigate the effects of eccentric loading on medium-size concrete columns internally reinforced with longitudinal and transverse steel bars and externally confined with SMA wires, and compare its behaviour with identical unconfined RC columns and with conventional CFRP-confined RC columns.

3. Literature review

Almost all compression members in concrete structures are subjected to moments in addition to axial loads. These may result from the columns resisting a portion of the unbalanced moments at the ends of the beams supported by the columns, or may be due to the load not being centered on the columns. An eccentrically loaded column experiences lateral deflection causing an increase in the column moments. These increased moments cause an increase in deflections, which in turn lead to an increase in moments. Because of the increase in maximum moment due to deflections, the axial load capacity of the column is decreased.

The confinement of concrete using FRP sheets has been proven experimentally and numerically to enhance the performance of the concrete [10–23]. The experimental research investigations conducted on passively FRP-confined columns showed column slenderness and load eccentricities have an important and detrimental effects on the effectiveness of FRP confinement [24–31]. The column slenderness and load eccentricities are also expected to reduce the effectiveness of actively SMA-confined columns. However, to date, no experimental testing has been performed to verify and quantify the effects of eccentric loading on the performance of SMA-confined RC columns.

Limited experimental data are available in the literature that provide an insight into the performance of SMA-confined concrete subjected to axial loads. The conceptual idea of utilizing the Shape Memory Effect (SME) phenomenon of the SMA as a confinement strategy to enhance the performance of the concrete was first proposed in the year 2000 by Krustulovic-Opara and Thiedeman [32]. This innovation comprised of embedding post-tensioned SMA fibres in the cementitious composites of high and normal-strength concrete cylinders. The test results reported in this study showed enhancements in the strength and ductility of the tested cylinders. Through the aforementioned study, Janke et al. [5] realized the potential of utilizing SMA as a form of external strengthening strategy to actively confine the concrete. Experimental investigation of this concept was first performed by Choi et al. [7], where the authors studied the ability of Nickel-Titanium (*NiTi*) SMA in the form of martensitic and austenitic wires to externally confine small-scale concrete cylinders. The findings reported in their study were considered a major breakthrough as it verified experimentally the success of concrete confinement using SMA wires, by quantifying the enhancement in the structural performance of the SMA-confined concrete. The effectiveness of utilizing *NiTi* SMA wires to actively confine concrete cylinders was further studied by several researchers [8,9,32–39]. The findings of these studies also confirmed the superior performance of concrete specimens confined with SMA wires, compared to their identical unconfined specimens.

The use of Nickel-Titanium-Niobium (*NiTiNb*) SMA wires was investigated by Choi et al. [7] to externally confine concrete cylinders. The test data showed that the *NiTiNb*-SMA wires increased the compressive strength and ductility of the concrete cylinders. They also found the specimens confined with *NiTiNb*-SMA wires were more effective in increasing the peak strength and dissipating more energy than the specimens confined with *NiTi*-SMA wires. Further experimental investigation was conducted by Shin and Andrawes [9], where the research focus aimed at comparing the performance of *NiTiNb*-SMA-confined concrete cylinders with cylinders wrapped with the conventionally used Glass-FRP (GFRP) sheets. The test results showed a significant increase in the strength and ductility of the actively SMA-confined cylinders over the GFRP-wrapped concrete cylinder. The authors also proposed a new hybrid active/passive confinement comprised of SMA spiral wires and GFRP/epoxy sheets (SMA-GFRP). The study showed that the hybrid SMA-GFRP confinement technique exhibited a superior performance over the passive GFRP confinement system, but did not attain the high ductility response observed by the concrete cylinders confined only with SMA wires. This research study clearly showed the potential of using SMA spirals solely or as a supplementary confinement technique along with FRP wraps. Finally, Tran et al. [37] conducted a similar research investigation as Choi et al. [33], where concrete cylinders were actively confined using *NiTi*-SMA wires in its martensite state, and passively confined using *NiTi*-SMA wires in its austenitic state. Their results clearly demonstrated the increase in the strength and ductility of the concrete to be more pronounced for active SMA-confinement, compared to the passive SMA-confinement.

The aforementioned studies demonstrated the effectiveness of the SMA wires to enhance the strength and ductility of the concrete. These studies also revealed the available experimental data for concentric loading of SMA-confined concrete columns suffer from one or more of the following shortcomings:

1. The number of test specimens were very limited due to the high cost involved with the *NiTi*-SMA wires. This leads to obtaining experimental data that lack statistical reliability;
2. The majority of the specimens tested were unrealistically short concrete cylinders and do not contain internal steel reinforcement;
3. The research studies mainly focused on investigating particular types of SMA (*NiTi*, *NiTiNb*) wires, rather than a systematic type approach that leads to a comprehensive understanding of the behaviour of SMA-confined concrete columns.

4. Objectives

In light of the above-mentioned discussion, this research project aims to avoid the shortcomings that currently exist in the available experimental data related to the concentric and cyclic behaviour of SMA confined concrete, and to provide new insights into the behaviour of SMA-confined concrete columns subjected to eccentric loading. The objectives of the current research program were:

1. To investigate experimentally the strength and deformability of SMA-confined RC columns subjected to varying uniaxial eccentric compressive loads;
2. To compare the axial-flexural behaviour of the SMA-confined RC columns with nominally identical unconfined RC columns, and RC columns confined with conventionally used CFRP sheets;
3. to present critically needed experimental data to understand the overall performance of actively SMA confined RC columns, and to add valuable experimental data to the relatively limited investigations conducted on eccentric loading of CFRP-confined RC columns.

5. Experimental investigation

5.1. Test matrix

The experimental program consisted of thirty-six circular RC

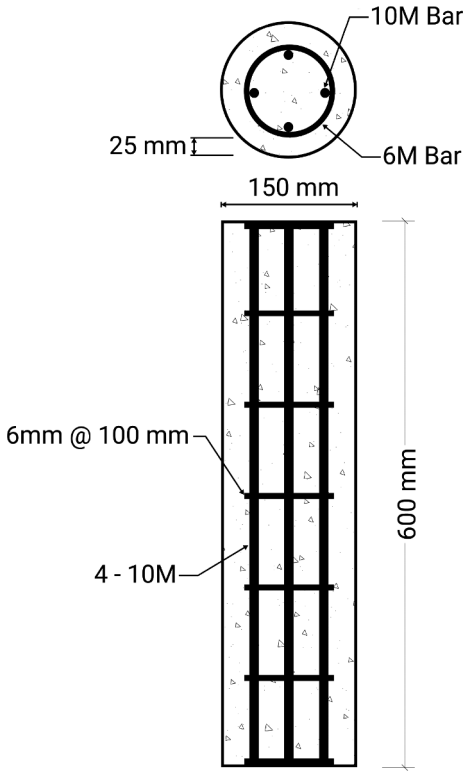

Fig. 1. Geometry of test specimens.

columns with identical aspect ratio (aspect ratio $H/D = 4$, where H and D refer to the height and diameter of the column, respectively), which were tested to failure under monotonic eccentric axial compressive load. The dimensions of the fabricated columns were 150 mm in diameter and 600 mm in height, and the columns were internally reinforced with four 10 M (nominal diameter of 11.3 mm) longitudinal steel bars and laterally reinforced with 6 mm diameter circular steel ties spaced at 100 mm centre-to-centre (Fig. 1).

Details of the test matrix are provided in Table 1. The test matrix was designed mainly to investigate two parameters, namely the presence of the confinement material (unconfined, CFRP sheets, and SMA wires), and the loading eccentricity (0D, 0.1D, 0.2D, and 0.3D, which corresponds to 0 mm, 15 mm, 30 mm, and 45 mm, respectively). The test specimens were divided into three groups, where each group consisted of twelve columns. The first group was left unconfined to act as control specimens, the second group was confined with one layer of the conventional CFRP sheets, and the third group was confined with SMA wires at a pitch spacing of 10 mm.

Table 1
Summary of test matrix.

	Column Type		
	Control	CFRP	SMA
No. of FRP Layers	–	1	–
SMA Pitch Spacing (mm)	–	–	10
Eccentricity	***No. of Specimens***		
0 mm	3	3	3
Specimen ID	*CT-0-Sp1/2/3*	*CFRP-0-Sp1/2/3*	*SMA-0-Sp1/2/3*
15 mm	3	3	3
Specimen ID	*CT-15-Sp1/2/3*	*CFRP-15-Sp1/2/3*	*SMA-15-Sp1/2/3*
30 mm	3	3	3
Specimen ID	*CT-30-Sp1/2/3*	*CFRP-30-Sp1/2/3*	*SMA-30-Sp1/2/3*
45 mm	3	3	3
Specimen ID	*CT-45-Sp1/2/3*	*CFRP-45-Sp1/2/3*	*SMA-45-Sp1/2/3*

The specimen ID shown in Table 1 can be described as follows: the first letters represent the confining material ("CT" for control specimens, "CFRP" for CFRP sheets, and "SMA" for SMA wires), followed by the number representing the eccentricity dimension (0 mm, 15 mm, 30 mm, and 45 mm), and the last digit (Sp1/2/3) indicates the specimen number within the same group. Three specimens were tested for each loading configuration to verify repeatability of the test results.

5.2. Constituent materials and ancillary testing

The test specimens were constructed using basic materials that were: normal density concrete, longitudinal steel bars, circular steel ties, CFRP sheets and SMA wires. The specimens were cast in three batches with a specified design concrete strength of 30 MPa. The type of CFRP sheet used in this study was SikaWrap Hex 230C with a ply thickness of 0.381 mm [40]. The adhesive system used to bond the CFRP sheet to the concrete surface consisted of two-component epoxy resin [41]. A summary of the constitutive material properties reported by the manufacturers and verified through ancillary testing for the concrete, longitudinal steel bars, circular steel ties, CFRP sheets and epoxy is summarized in Table 2.

In general, the results show that the ancillary tests agree well with the reported manufacturer data for verification purposes. Variations in the tensile properties between nominally identical specimens of the CFRP coupon samples resulted in relatively high standard deviation values. This is caused by the difficulty involved with the preparation procedure of the coupon sample, specifically related to impregnating the CFRP sheets with epoxy and ensuring that the CFRP laminate has the exact thickness as that reported by the manufacturer, for comparison purposes. Further variables contributing to the variation of the test results include the accuracy involved with the loading alignment of the very slim CFRP coupon sample, and the measurement errors of the mounted strain gauges.

The SMA wires used in this study were of type Nickel-Titanium (*NiTi*) and had a round cross-sectional diameter of 1.9 mm [0.075 in]. The SMA wires were supplied by the manufacturer in a pre-strained condition that can provide a linear strain recovery up to 6.3% when heated above the A_s temperature of 60 °C. According to tensile tests performed by the authors [6], the SMA wires had a mean ultimate tensile strength of 1074 ± 8.8 MPa, and a strain at failure of 34 ± 3.6%. Based on the recovery stress test performed by the authors, the SMA wires had a maximum recovery stress of 581 MPa and a residual recovery stress of 485 MPa. Further information about the characterization and the material properties of the SMA wires can be found in Abdelrahman and El-Hacha [6].

5.3. Design philosophy

For comparison purposes, the experimental test program was designed to maintain an equivalent lateral confinement pressure between the SMA-confined columns and the CFRP-confined columns. The formulation of the equation to determine the lateral confinement pressure of a circular cross-section column wrapped with SMA wires and CFRP sheets are shown in Fig. 2. Based on equilibrium of forces and strain compatibility, the equations to determine the lateral confinement pressure (f_l) of the CFRP-confined columns and the SMA-confined columns are given by Eqs. (1) and (2), respectively.

$$f_l = \frac{2t_j f_j}{D} \tag{1}$$

$$f_l = \frac{2A_{SMA} f_{SMA}}{SD} \tag{2}$$

where, t_j and f_{ju} are the thickness and the ultimate tensile strength of the CFRP sheet; A_{SMA} and f_{SMA} are the cross-sectional area and the ultimate tensile strength of the SMA wire; S is the pitch spacing of the SMA wire

Table 2
Summary of the manufacturers reported data and the ancillary test results of the constitutive materials.

Material	ASTM Standard	Property		Manu.	Avg.	Std. Dev.	# of tests
Concrete	ASTM C39-C39M [42]	Compressive Strength	(MPa)	30	32.5[1]	1.5	3
					31.0[2]	1.3	3
					29.4[3]	0.7	3
6 M Steel	ASTM A370-17 [43]	Yield Strength	(MPa)	–	676	11.6	3
		Ultimate Strength	(MPa)	–	707	4.3	
10 M Steel	ASTM A370-17	Yield Strength	(MPa)	–	404	2.9	3
		Ultimate Strength	(MPa)	–	622	2.6	
CFRP Sheet	ASTM D3030/D3039M [44]	Tensile Strength	(MPa)	894	710	140	3
		Elastic Modulus	(MPa)	65,402	68,900	9.16	
		Rupture Strain	(%)	1.33	1.29	0.15	
		Thickness	(mm)	0.381	0.381	–	
Epoxy	ASTM D3030/D3039M	Tensile Strength	(MPa)	30	–	–	–
		Elastic Modulus	(MPa)	3.8			
		Strain at Failure	(%)	1.5			

1, 2, 3 = concrete batch #1, concrete batch # 2 and concrete batch # 3.
– = not provided/ non-measured items.
Manu. = manufacturer.
Avg. = average.

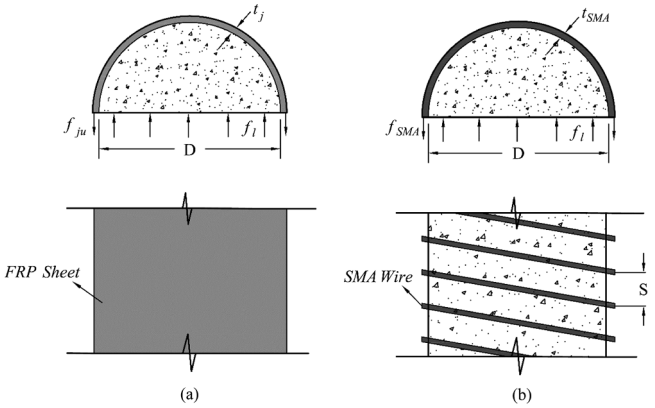

Fig. 2. Confinement parameters of (a) CFRP-confined and (b) SMA-confined columns.

and D is the diameter of the concrete column.

Based on the dimensions of the column and the mechanical properties of the strengthening materials (CFRP sheets and SMA wires) selected for this research investigation, the confinement pressure of the columns confined with a single layer of CFRP sheets (4.5 MPa) is almost equivalent to that of the columns confined with SMA wires at a pitch spacing of 10 mm (4.1 MPa). The selection of the pitch spacing of the SMA wires was deemed appropriate to minimize the loss in confinement due to the arching action in the area of concrete between the SMA spirals. The confinement pressure can be considered as a common base parameter for comparison purposes of the test data.

5.4. Specimen preparation

The CFRP sheets were applied to the concrete columns using the conventional wet-layup bonding procedure, as recommended by the manufacturer [40]. An additional layer of epoxy resin was added to the exterior of the CFRP sheets to ensure complete saturation of the fibres and full development of the composite strength. A circumferential overlap of 100 mm was used in all CFRP-confined specimens [40].

Spirals formed from SMA wires were used to confine the RC columns. For pre-straining and shipping purposes, the pre-strained martensitic SMA wires were supplied by the manufacturer [45] in cut lengths of 2.4 m. Therefore, a splicing technique was developed which consisted of four U-clamp anchors to connect the SMA segments and develop the full length of the spirals (Fig. 3). The ends of the SMA spiral were constrained to the concrete column by coiling the SMA wires with two additional turns and secured to the concrete column using U-clamp anchors. The martensitic state of the SMA wires allows for flexibility and ease of operation during the confinement process. The confining spirals were formed by circumferentially wrapping the SMA wires under a constant tensile force at a pitch spacing of 10 mm. A typical SMA-confined RC column is shown in Fig. 3.

The process of actively confining the RC column was initiated by connecting the ends of the SMA spiral to an electrical circuit. The pre-strained SMA spirals were then heated by passing an electrical current to activate the shape recovery mechanism. Since the ends of the SMA spirals were constrained to the concrete column, a confining pressure was generated as the SMA wire transformed from a martensitic state to an austenitic state while trying to achieve a zero-strain condition. The active confinement procedure was completed once the temperature of the SMA spirals reached 120 °C because this ensured complete transformation of the SMA wires from a martensitic state to an austenitic state. Further information regarding the active confinement procedure of the SMA-confined specimens can be found in Abdelrahman and El-Hacha [6].

5.5. Instrumentation and test set-up

The detailing of the column instrumentation is illustrated in Fig. 4. The tested columns were externally instrumented at their mid-heights with four Pi-type strain gauges (gauge length of 150 mm) in the axial direction and with two conventional electrical foil strain gauges (gauge length of 6.35 mm) in the hoop direction. The lateral deflections along the height of the tested columns were monitored using three Linear Strain Convertors (LSC) and three Laser Displacement Sensors (LDS) as shown in Fig. 4. The vertical deflections were monitored using two LSC's mounted at the bottom end of the columns.

The internal longitudinal steel reinforcement was also instrumented with four conventional foil strain gauges at the mid-height of the columns. Two strain gauges were installed vertically onto the longitudinal reinforcement to measure the localized axial strains (gauge length of 6.35 mm), and two strain gauges were installed onto the circular ties horizontally to measure the localized hoop strains (gauge length of 3.18 mm). The strain gauges were mounted to the steel reinforcement on two opposite sides as illustrated in Fig. 4.

Prior to loading the concrete column, the ends of the columns were confined with steel collars to avoid premature failure of the concrete.

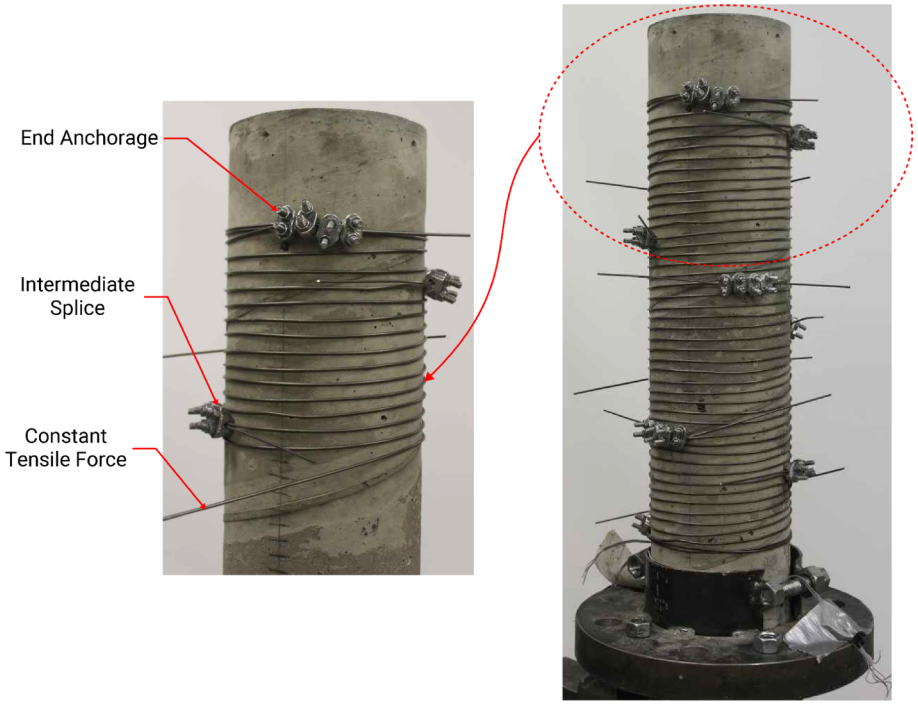

Fig. 3. Typical SMA-confined RC column.

All columns were tested under pinned-end conditions to account for extreme bending moment scenarios. Special end loading plates were fabricated to enforce pinned-end conditions and allow for the application of concentric and eccentric loading conditions. The design of the loading plates included two rectangular steel plates; a top loading plate (300 mm × 450 mm × 25 mm thick) and a bottom loading (300 mm × 300 mm × 25 mm thick) plate. In between the plates, a roller (50 mm in diameter) was welded to the top loading plate and fitted into the grove that was machined into the bottom loading plate (Fig. 5). The bottom loading plate consisted of a larger rectangular section to accommodate the varying eccentric locations of the columns. A spherical seat was mounted to the loading plates to rule out of planarity errors found at the column's end surface (Fig. 5).

The selection of the eccentricity distances was based on percentage values of the column diameter (D). The range of eccentricity distances selected were 0D, 0.1D, 0.2D, and 0.3D, which corresponds to 0 mm, 15 mm, 30 mm, and 45 mm, respectively. The range of the load eccentricity distances was selected to enable the generation of load-moment (P-M) interaction diagrams for unconfined, CFRP-confined and SMA-confined RC columns. All columns were tested to failure under

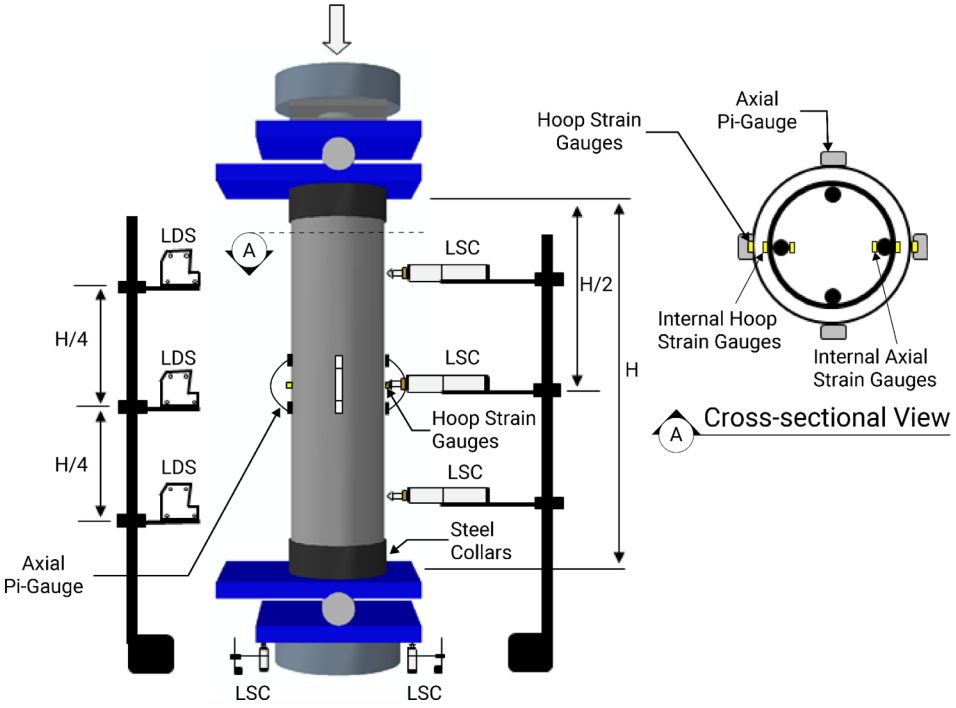

Fig. 4. Instrumentation of test specimens.

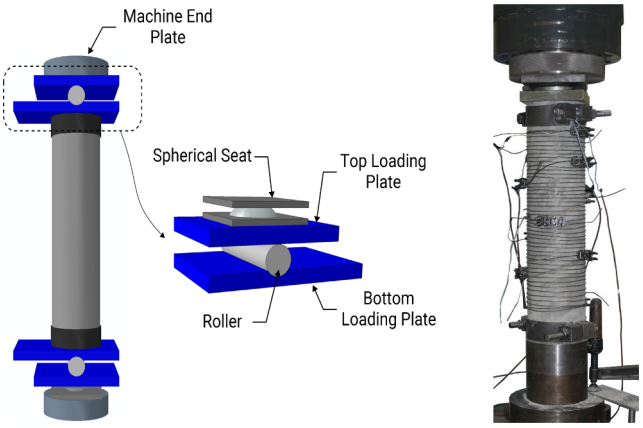

Fig. 5. Test set-up of the RC columns.

uni-axial compressive loads with MTS load frame compression machine (capacity of 2 MN) in a displacement control mode at a rate of 0.5 mm/mm (Fig. 5).

6. Results and discussion

6.1. Failure mode

The failure pattern for all unconfined RC specimens was typical. At early stages of loading, tensile cracks were formed on the tensile face and propagated as the load increased. A drop in the load was observed when the concrete on the most compressed face of the column was crushed/spalled, accompanied in many cases by buckling of the most compressed longitudinal reinforcement (Fig. 6a).

The failure mode of all CFRP-confined RC columns initiated with cracking noises heard during the early stages of loading attributed to the microcracking of the concrete. At loads corresponding to their nominally identical unconfined concrete column strength, cracking noises from the CFRP sheets was obvious indicating the activation of the passive confinement mechanism. The failure of all CFRP-confined columns was sudden and characterized by rupture of the CFRP sheets followed by shattering of the already crushed concrete. As expected, the CFRP-confined columns subjected to concentric loading (zero eccentricity) experienced the most catastrophic failure. As the load eccentricity increased, the curvature of the specimens was visible and the maximum lateral deflection was observed at the mid-height region of the column. The failure was localized towards the most compressed side of the column. Inspection of the failed specimens showed buckling of the longitudinal reinforcement at the most compressed face of the columns (Fig. 6b). The inspection also revealed that chunks of concrete remained attached to the ruptured CFRP sheets demonstrating the good bond performance between the CFRP sheets and the concrete surface.

During testing, all SMA-confined RC columns experienced significant cracking and crushing of the concrete. These cracks initiated at the mid-height region of the SMA-confined columns subjected to concentric loading (e = 0 mm) and then progressed diagonally to both ends of the specimen as shown in Fig. 6c. Eccentrically loaded SMA-confined RC columns displayed high curvatures and lateral deflections accompanied with excessive concrete cracking, eventually leading to tensile fracture of the SMA wires at the mid-height region of the columns. The SMA wires rupture occurred at the most compressed face of the column along with buckling of the longitudinal reinforcement. Inspection of the failed specimens showed the SMA-confined columns remained intact despite the high axial and lateral deformations recorded. The reason is attributed to the active confinement pressure applied by the SMA spirals.

A comparison between the failure modes of the passive CFRP-confinement system and the active SMA-confinement system shows that the extent of the damage sustained by the SMA-confined RC columns was relatively small compared to the CFRP-confined RC columns at similar stress levels. This demonstrates the effectiveness of the SMA spirals to actively confine the concrete by controlling the cracking and delaying the failure of the column.

6.2. Load-displacement behaviour

The load (P) - displacement (Δ) curves for the tested specimens are shown in Fig. 7. The longitudinal deflections (U_{Long}) were measured using LSC's mounted to the testing actuator and the lateral deflections (U_{Lat}) were obtained from the mid-height LSC and LDS. It should be noted that each curve shown in Fig. 7 is an average response from three nominally identical specimens. The results of the individual specimens in terms of the yield load and maximum load are summarized in Table 3, and the load-displacement responses of the individual specimens can be found in Abdelrahman [46]. The P-Δ responses of all unconfined specimens (Fig. 7) exhibited a curvilinear behaviour characterized by an approximate linear load-longitudinal/lateral behaviour up to the yield point. The yield point corresponds to the yielding of the compression bars in the case of the unconfined columns subjected to eccentric loading at distances less than 0.2D (e = 30 mm), and corresponds to the yielding of the tension bars in the case of the unconfined columns subjected to load eccentricity greater than 0.2D. After the yield point, the stiffness of the columns decreased due to excessive concrete cracking until a peak load is reached. The peak points of the curves denote failure of the columns by concrete crushing and buckling of the longitudinal steel at the most compressed face of the column. Subsequently, a drastic reduction in the stiffness and load capacity of the column was observed with increasing lateral and axial deformations. The testing was eventually terminated when the load capacity dropped to about 10% of the column strength. It is important to note that the yielding of the longitudinal steel reinforcement was determined by stain gauges mounted in the vertical orientation to measure axial strains.The P-Δ responses of the CFRP-confined RC columns were considerably affected by increasing load eccentricity based on Fig. 7. All CFRP-confined RC columns displayed linear response up to a yield point. The yield point and the post-yield behaviour critically relies on the level of load eccentricity applied to the column. For the columns subjected to load eccentricities at distances less than 0.2D (e = 30 mm), the yield point of the P-Δ response curve occurred when the longitudinal bars at the most compressed face of the column started yielding. Subsequent lateral expansion beyond the yield points induced large tensile forces on the CFRP sheets. The CFRP sheets were then activated to resist the lateral expansion of the concrete. The concrete column becomes confined under a tri-axial state of stress leading to enhancements in the strength and deformation. This stage was represented by a linear increasing branch until failure denoted by tensile rupture of the CFRP sheets at the most compressed face of the column. For the columns subjected to load eccentricity greater than 0.2D, the yield point of the P-Δ response corresponded to the yielding of the tension bars. After the yield point, the stiffness dropped significantly due to excessive concrete cracking. At this stage, the CFRP sheets were activated forming a yield plateau with slight increase in the strength as the axial and lateral deformations of the column increased. This eventually lead to the failure of the column by the fracture of the CFRP sheets at the most compressed face of the column.Examination of the P-Δ responses of the SMA-confined specimens (Fig. 7) show the columns exhibited a curvilinear behaviour with increasing axial and lateral deformations. Similar to the CFRP-confined specimens, a linear response was observed for the SMA-confined RC columns up to a yield point. The P-Δ responses following the yield point displayed a softening stage with a gradual increase in the load and the longitudinal/lateral deformations up to a peak point. After the peak point, the stiffness significantly decreased for the columns subjected to eccentric loads at distances less than 0.2D, whereas a gradual decrease in the stiffness was observed for

Fig. 6. Failure modes of unconfined, CFRP-wrapped, and SMA-confined RC columns tested at e = 0 mm, e = 15 mm, e = 30 mm, and e = 45 mm.

columns subjected to load eccentricity greater than 0.2*D*. The SMA-confined columns ultimately fail by fracture of the SMA wires at the most compressed face of the column.A comparison between the *P*-Δ responses of all tested specimens show that the unconfined RC columns were drastically affected by increasing load eccentricities and their axial and flexural capacity are extremely limited. As expected, the confinement of concrete with passive CFRP sheets and active SMA spirals significantly enhanced the axial and flexural capacity of the concrete columns. This is further illustrated in Fig. 8, which shows the maximum load attained by the column normalized to the unconfined concentric case in relation to the initial load eccentricity. The figure shows the load capacity of the CFRP-confined RC columns and the SMA-confined concrete columns increased by up to 70% and 55%, respectively, compared to unconfined RC columns. It should be noted that the amount of confining pressure, whether passive or active, was employed as the common base for comparison. As discussed earlier, the total confining pressure applied in the case of the passive CFRP-confined RC columns wrapped with one layer of CFRP sheets was 4.5 MPa, whereas the total confining pressure applied in the case of the RC columns actively confined with SMA spirals at 10 mm pitch spacing was 4.1 MPa. This explains why the SMA-confined RC columns had lower load capacity (by 10%) compared to the CFRP-confined RC columns, which is directly related to the percentual difference (10%) in the confining pressure between the active SMA-strengthening and the passive CFRP-strengthening system.The results plotted in Fig. 8 also show enhancements in the peak load for CFRP-confined and SMA-confined RC columns were realized even at high eccentricity levels of 0.3*D* (45 mm), where a 50% increase in the axial strength was found over nominally identical unconfined columns. Even though the load capacities of the confined (CFRP and SMA) columns were always greater than their equivalent unconfined columns, the reduction in the strength was pronounced in the case of the confined columns with the increase in the

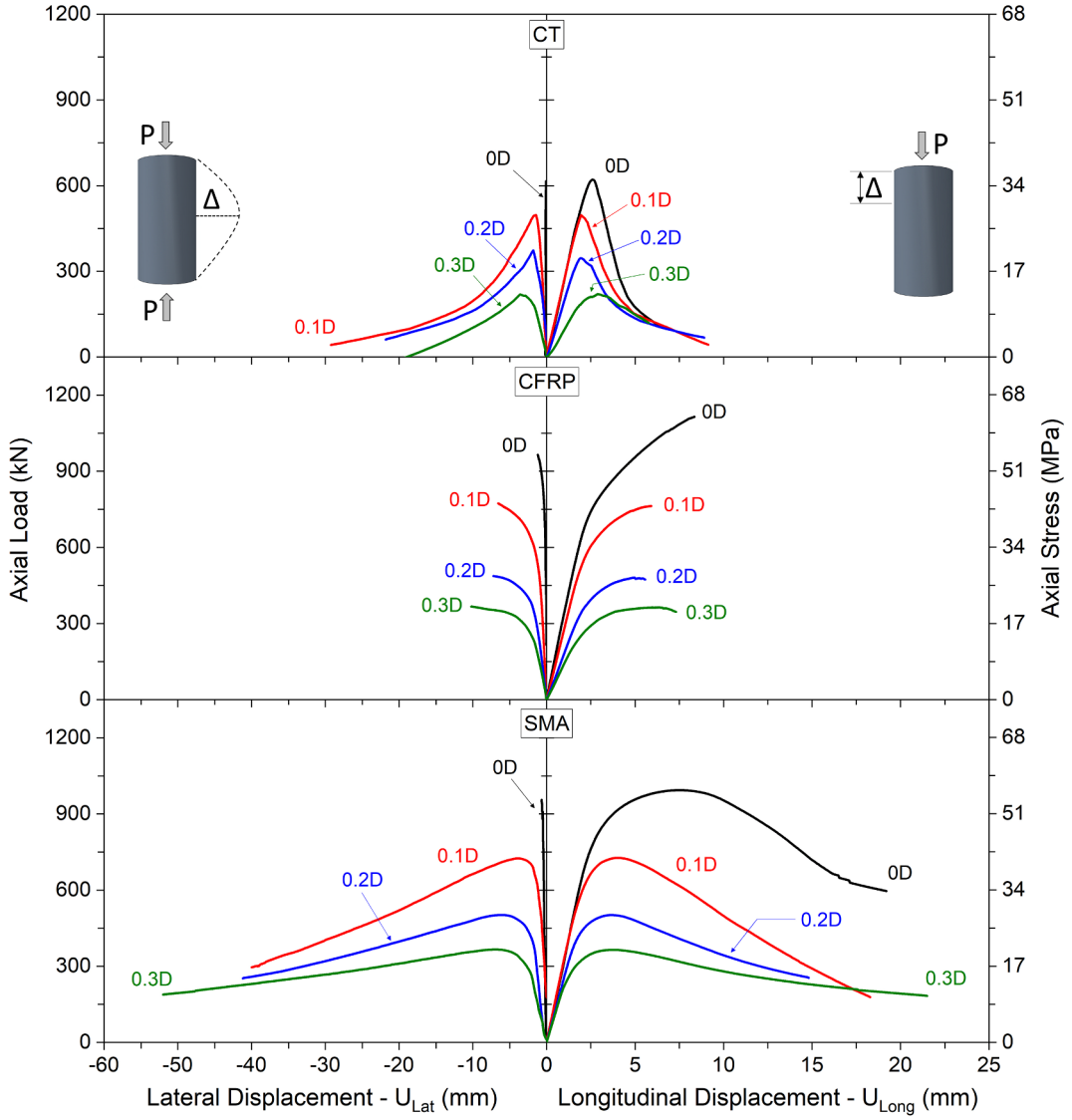

Fig. 7. Load-displacement behaviour of unconfined RC columns, CFRP-confined RC columns and SMA-confined RC columns.

Table 3
Summary of test results.

Specimen ID	Peak Axial Load (kN)	Avg. Axial Strain at Peak[(b)] (%)	Max. Comp. Axial Strain at Peak (%)	Comp. Axial Strain at Ultimate (%)	Max/Ult. Hoop Strain at Comp. Face (%)	Yield Load (kN)	Yield Axial Strain at the Comp. Face (%)	Yield Hoop Strain at the Comp. Face (%)
CT-0D	638 ± 11	0.15 ± 0.02	0.22 ± 0.007	NA[a]	0.21 ± 0.07	620 ± 20	0.14 ± 0.02	0.14 ± 0.03
CFRP-0D	1085 ± 52	0.73	1.13 ± 0.08	NA	0.79 ± 0.2	724 ± 21	0.33 ± 0.1	0.047 ± 0.008
SMA-0D	995 ± 17	0.62	1.10 ± 0.1	2.56 ± 0.2	2.67 ± 0.6	775 ± 23	0.14 ± 0.02	0.034 ± 0.01
CT-0.1D	517 ± 27	0.093 ± 0.009	0.27 ± 0.05	NA	0.32 ±	422	0.19	Damaged
CFRP-0.1D	761 ± 22	0.35 ± 0.03	1.14 ± 0.01	NA	0.76 ± 0.06	486 ± 16	0.19 ± 0.001	0.068 ± 0.02
SMA-0.1D	729 ± 21	0.31 ± 0.1	0.90 ± 0.2	2.57 ± 0.2	1.98 ± 0.7	528 ± 45	0.19	0.043 ± 0.02
CT-0.2D	389 ± 6	0.056 ± 0.02	0.37 ± 0.1	NA	0.75 ± 0.4	326 ± 38	0.45 ± 0.06	0.048 ± 0.02
CFRP-0.2D	492 ± 18	0.15 ± 0.02	1.5 ± 0.1	NA	0.81 ± 0.2	336 ± 55	0.29 ± 0.07	0.097 ± 0.02
SMA-0.2D	503 ± 11	0.19 ± 0.08	0.97 ± 0.1	3.65 ± 1.7	0.92 ± 0.2	398 ± 3	0.28 ± 0.03	0.056 ± 0.02
CT-0.3D	246 ± 3	0.026	0.36	NA	0.13 ± 0.06	240 ± 3	0.22	0.15 ± 0.06
CFRP-0.3D	364 ± 25	0.08 ± 0.02	1.46 ± 0.3	NA	0.59 ± 0.01	299 ± 16	0.11	0.43
SMA-0.3D	371 ± 19	0.28	0.79	4.9	1.9	327 ± 40	Damaged	0.15

eccentric distance of the applied load. For instance, increasing the load eccentricity from 15 mm (0.1*D*) to 30 mm (0.2*D*) reduced the load capacity of the strengthened columns by 55%, compared to the unconfined columns that experienced a 33% reduction in the load capacity.Further examination of the *P*-Δ responses plotted in Fig. 7 show the SMA-confined RC columns displayed a stiffer linear elastic response up to the yield point compared to the CFRP-confined RC columns. This behaviour is attributed to the active confinement pressure applied by the SMA spirals which acted to restrain the lateral expansion of the column during the initial loading stages compared to the CFRP jackets

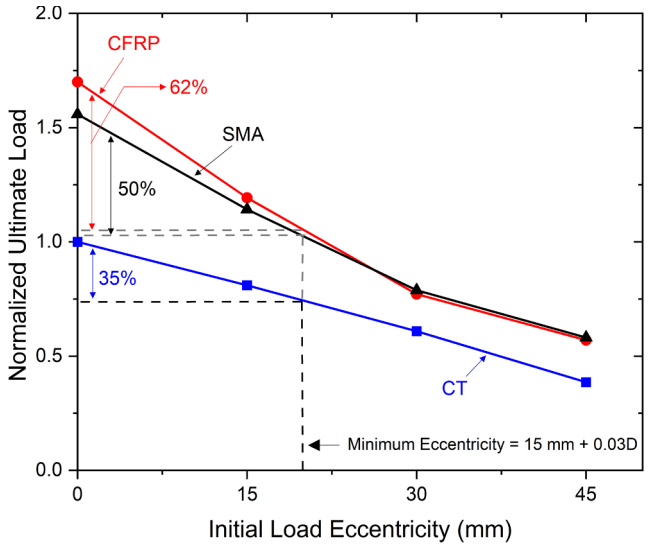

Fig. 8. Normalized ultimate load capacity vs. initial load eccentricity.

which were activated passively after the concrete experienced significant damage and lateral expansion. The results also show that even after the concrete experienced severe damage, the SMA spirals were able to sustain as high as 93% (at $e = 0D$) and as low as 35% (at $e = 0.1D$) of the concrete peak strength at failure. This demonstrates the effectiveness of the active confinement applied by the SMA spirals to restrict the opening and propagation of concrete cracking until the failure point.

6.3. Minimum load eccentricities

The maximum strength predicted theoretically cannot be normally attained by the concrete columns because there is always some form of unavoidable moments or eccentricities applied to the columns. These moments or eccentricities can occur due to misalignments of columns from floor to floor, misalignments of the internal steel reinforcement, unbalanced moments in the beams/slabs, or uneven compaction of the concrete across the width of the section [47]. As shown in Fig. 8, the application of the load at an eccentric distance adversely impacts the load carrying capacity of the columns.

To account for the effect of accidental or unanticipated moments, the CSA A23.3-04 CL. 10.10.4b [48] specifies the maximum load

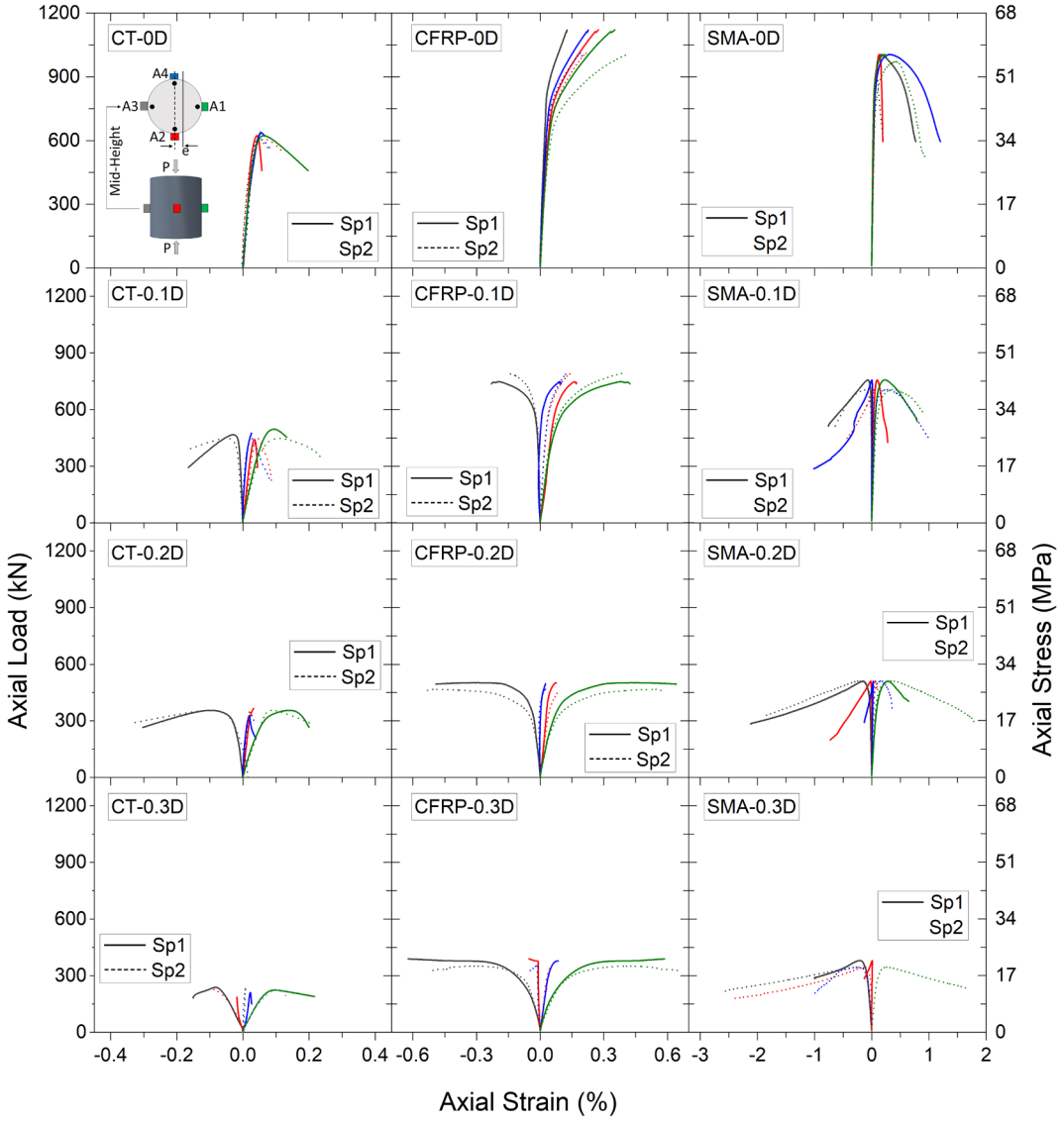

Fig. 9. Load vs. axial strain behaviour of unconfined RC columns, CFRP-confined RC columns and SMA-confined RC columns.

applied on the tied column be limited to 80% of its column capacity P_{ro} ($0.8P_{ro}$). The CSA A23.3 CL.10.15.3.1 defines the minimum eccentricity (e_{min}) as a function of the column thickness (h) as $e_{min} = 15\text{ mm} + 0.03\,h$, which corresponds to 19.5 mm for the columns tested in the current study. The results presented in Fig. 8 shows a 35% reduction in the load capacity of the column at the minimum load eccentricity ($\boldsymbol{e_{min}} = 19.5$ mm), whereas the CFRP-confined and the SMA-confined RC columns experienced a 62% and 50% reduction in the load capacity, respectively. These results clearly indicate the eccentricity effects are more detrimental on externally CFRP/SMA-confined RC columns, in comparison to the unconfined RC columns. The code-specified reductions of 20% to the column capacity to account for minimum eccentricity seem slightly unconservative for the unconfined columns and highly unconservative for the CFRP-confined and the SMA-confined RC columns.

In the recent edition of the CSA A23.3-14 [49], the limitation on the maximum load (P_{rmax}) to account for the minimum load eccentricity was modified from a fixed reduction of 20% ($0.8P_{ro}$) to an equation that relies on the column thickness defined in Clause 10.10.4b as:

$$P_{r\max} = [0.2 + 0.002\,h]\,P_{ro} \tag{3}$$

According to CSA A23.3-14, the maximum applied load on the columns tested in the current study is limited to 50% of its column capacity. The results observed in Fig. 8 show the modified code-specified reductions of 50% to the column capacity to account for minimum eccentricity is conservative in the case of the unconfined RC columns (35%) and slightly unconservative in the case of the CFRP-confined (65%) and SMA-confined RC columns (50%). Thus, it is imperative further research studies be conducted on the load eccentricity effects of externally confined RC columns to conservatively estimate load limitations factors to account for minimum load eccentricity.

6.4. Axial and hoop strain

The load versus axial strain responses for the unconfined, CFRP-confined, and SMA-confined RC columns are presented in Fig. 9. For clarity purposes, the load versus hoop strain responses for only one specimen per load configuration are plotted in Fig. 10. Full details of the recorded load versus hoop strain behaviour for all specimens can be found in Abdelrahman [46]. A complete summary of the test data is presented in Table 3, which includes the average axial strain corresponding to the peak load, the axial and hoops strains at maximum and ultimate loads, and hoop and axial strains recorded at the yield point of the column.

It is worth mentioning that, in many cases, specifically for the unconfined and the SMA-confined RC columns, the strain gauges and Pi-gauges installed to capture the hoop strains and axial strains responses, respectively, were either debonded or damaged/malfunctioned prior to the failure point. The reason is that the strain measurement instrumentations for these specimens were mounted directly onto the concrete surface that undergoes excessive cracking at loads close to failure resulting in debonding or damaging/malfunctioning of the strain gauges and Pi-gauges. It is important to understand that the strain data presented in Fig. 9, Fig. 10 and Table 3 do not necessarily correspond to the maximum/ultimate conditions, but may also represent the final strain recorded prior to damage/malfunction of the strain gauge/Pi-gauge. However, the axial strain and hoop strain data captured were sufficient to provide general observations and conclusive trends discussed in this section.

Examination of the load versus axial strain behaviour for the unconfined, CFRP-confined, and SMA-confined RC columns (Fig. 9) showed the bending moment induced by the eccentric loading and increasing secondary moments resulted in an axial strain gradient along the column cross-section with both compressive and tensile strains. The variation in the axial strains was even recorded in the concentrically loaded columns suggesting that a pure concentric load case was not

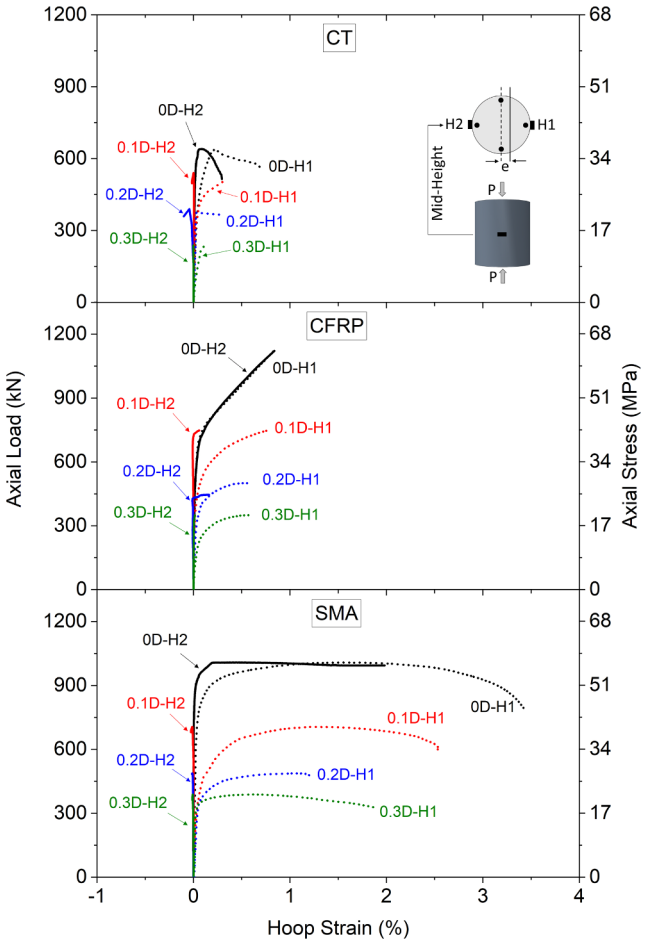

Fig. 10. Load vs. hoop strain behaviour of unconfined RC columns, CFRP-confined RC columns and SMA-confined RC columns.

achieved. The axial strain readings presented in Fig. 9 also show a minor skewness on opposite strain gauge readings at the location of the neutral axis indicating that columns may have experienced accidental biaxial bending. This is not considered significant and is believed to have minimum impact on the test results presented herein. Inevitable eccentric or biaxial loads may have occurred due to the following reasons; (1) unforeseen error in the alignment of the loading apparatus; or (2) misalignment of the tested columns; or (3) inherent variability in the concrete.

The load versus axial strain behaviours (Fig. 9) typically shows axial strains at the most compressed face of the column demonstrated a response similar to their corresponding load versus longitudinal displacement behaviour (Fig. 7). Further examination of the load versus axial strain data recorded in Table 3 shows the average axial strain at peak (the average strain is calculated from the four Pi-gauges located at the mid-height of the column) for the unconfined, CFRP-confined, and SMA-confined RC columns drastically decreased with increasing column eccentricity. This behaviour is expected since increasing column eccentricity globally reduces the portion of the concrete subjected to compressive stresses. This results in a significant reduction in the effectiveness of the confinement material (CFRP sheet and SMA wire) as the confining benefits are only realized at the most compressed face of the column.

It is apparent in Table 3 the compressive axial strains corresponding to the maximum and ultimate loads increase with increasing eccentric loading. This observation contradicts the trend recorded by the average axial strains discussed earlier. It is important to recognize that the average axial strain represent the overall compressive global response

of the specimen. The increase in the applied load eccentricity reduces the global compression state of the column and transfers the response from an axial load dominated response to a flexural dominated response. The compressive axial strains at maximum/ultimate loads located at the most compressed face of the column represents a localized behaviour and the enhancement observed in the recorded axial strains with increasing eccentric loading is termed by a few researchers as the axial strain enhancement phenomenon [25,26,29]. This phenomenon describes the redistribution of the uneven dilation occurring at the highly compressed face of the column to the global cross-section. This redistribution allows the highly compressed region of the column to further deform axially prior to achieving the failure strain of the confining material.

The load versus hoop strain response plotted in Fig. 10 shows the bending moments caused by the eccentric compressive loads resulted in tensile hoop strains at the most compressed face of the columns and almost minimal or slightly compressive strains at the least compressed end. Tensile hoop strains are only observed at the most compressed side of the column because this region experiences dilation that activates the confining material. It is important to restate that the maximum/ultimate hoop strains reported in Table 3 represent in most cases the final strain reading prior to the damage/malfunction of the strain gauge and do not necessary reflect maximum/ultimate conditions. A general observation regarding the hoop strain response can be deduced from Table 3, while considering the axial strain data and the visual laboratory observations. It is expected that the hoop strains at maximum/ultimate loads increase with large eccentricities due to the higher localized dilation at the most compressed face of the column. This trend was exhibited by the unconfined and CFRP-confined RC columns as shown in Table 3, but was not quantified for the SMA-confined RC columns as these columns experienced excessive deformation mentioned earlier, consequently damaging the strain gauges mounted onto the surface prior to failure.

A comparison between the load versus axial/hoop strain responses of all tested specimens show that the unconfined RC columns were drastically affected by the increase in the initial load eccentricity. Confining the RC columns with CFRP sheets and SMA wires enhanced the axial and hoop strain performance of the concrete significantly compared to the unconfined columns. The axial strains achieved at peak loads for the CFRP-confined and SMA-confined RC columns were higher by up to five times compared to the control specimens. The SMA-confined RC columns exhibited a post-peak response that allowed further axial deformation prior to failure resulting in an enhancement in the axial strain capacity of the column by up to 14 times and 3 times, when compared to the unconfined and the CFRP-confined RC columns, respectively.

It should be noted that the maximum hoop strains recorded at failure for the CFRP-confined RC columns were lower than the tested failure coupon strain. Previous research conducted by the authors [19,29] related to the strain measurement of FRP-confined concrete implementing the photogrammetric Digital Image Correlation (DIC) technique showed in many cases the maximum hoop strains that corresponded to the failure point occurred at regions not captured by the discrete foil strain gauges.

Further examination of the test data presented in Table 3 shows the axial strains at yield load for the CFRP-confined and SMA-confined RC columns were lower than those attained by their corresponding unconfined RC columns. This demonstrates the increased stiffness experienced by the confined columns that resulted in delaying the yielding of the steel reinforcement. The axial strains and hoop strains recorded at yield loads for the SMA-confined RC columns were in general lower than those achieved by their corresponding CFRP-confined RC columns. However, the yielding points of the SMA-confined columns were measured at higher loads (by up to 18%) compared to the CFRP-confined columns. The lower strains and higher loads at the yield point demonstrate the effectiveness of the SMA wires to actively confine

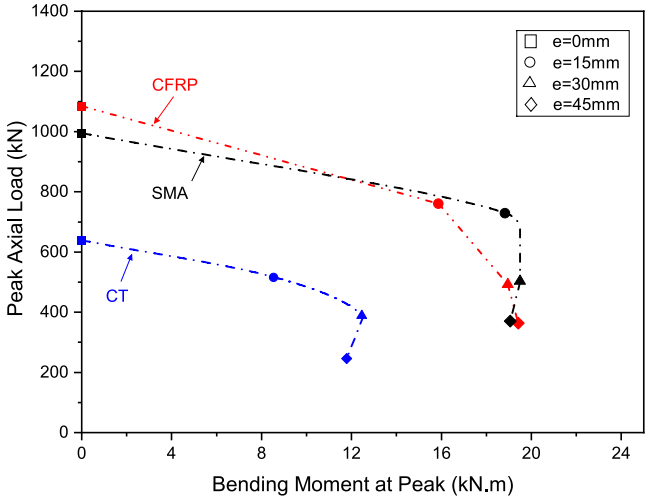

Fig. 11. Axial - flexural interaction of unconfined RC column, CFRP-confined RC columns and SMA-confined RC columns.

the concrete during the early stages of loading and increase the initial axial stiffness of the column in comparison to the passive CFRP-system that engages the CFRP sheet after significant dilation and damage is experienced by the concrete column. The effectiveness of the active SMA-confined system can be further demonstrated by the significantly higher axial strains and hoop strains attained at failure confirming the efficiency of the SMA spirals to control the opening and propagation of the concrete cracking.

6.5. Axial-flexural interaction

The recorded *P-M* responses for the tested unconfined, CFRP-confined and SMA-confined RC columns are plotted in Fig. 11. As noted above, the SMA-confined RC columns exhibit a ductile post-peak response. However, for comparison purposes, the interaction response of the tested specimens is plotted at the peak axial load and its corresponding bending moment at peak. The total bending moment (M) for the data in this figure includes the moments induced due to the initial load (P) eccentricity (e) and the secondary moments due to the lateral deflection at the mid-height of the column (Δ) corresponding to the peak load, evaluated as follows:

$$M = P(e + \Delta) \tag{4}$$

The results presented in Fig. 11 clearly demonstrate the confinement benefits using CFRP sheets and SMA wires which resulted in significant enhancement in the load carrying capacity and flexural capacity of RC columns under various eccentric loadings. As discussed earlier, the axial strength achieved by the CFRP-confined and the SMA-confined RC columns were relatively comparable because the axial stiffness of the columns was designed to provide similar properties to form a basis for comparison of the test results. The results indicate the SMA-confined RC columns exhibited a slightly higher load-moment interaction response at peak loads compared to the CFRP-confined RC columns.

It is also apparent in Fig. 11 the confinement benefits decrease past the balanced point as the columns transition from an axial load dominant state to a flexural dominant state. It is expected at high eccentric loads approaching the pure flexural case, the confinement benefits become negligible. Minimal enhancements in axial and flexural capacity of the columns are achieved through hoop confinement in a flexural-dominant loading condition.

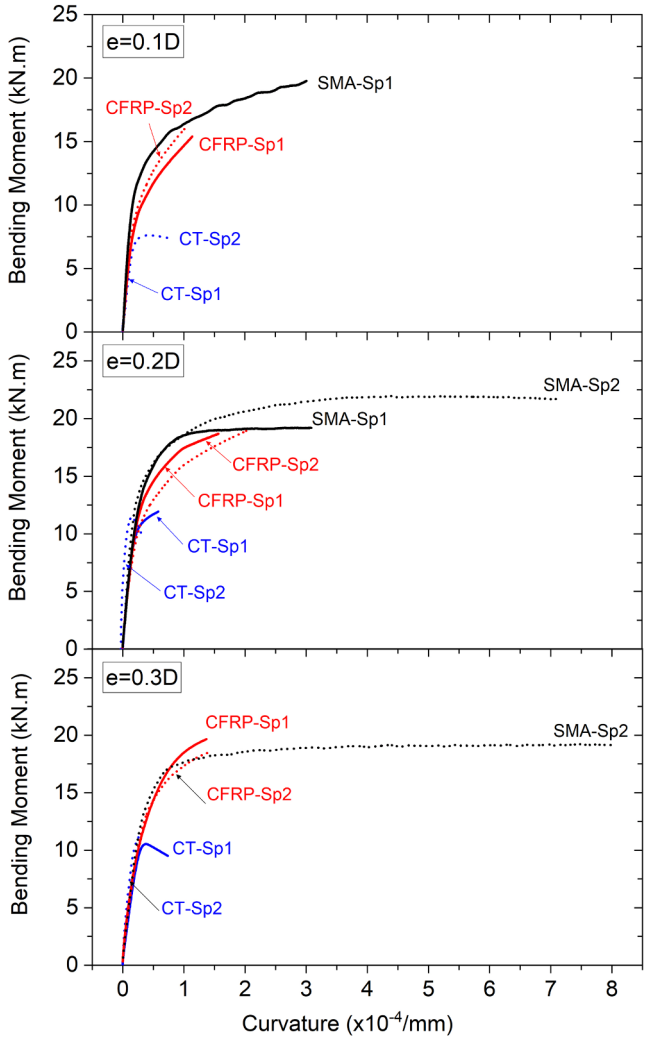

Fig. 12. Moment – curvature response of unconfined RC columns, CFRP-confined RC columns and SMA-confined RC columns.

6.6. Moment-curvature behaviour

The moment-curvature (M-φ) behaviour of the unconfined, CFRP-confined, and SMA-confined RC columns are shown in Fig. 12. The calculated bending moments included bending due to initial load eccentricity and secondary bending moments measured by lateral deflections at the mid-height of the specimen. The total bending moment was evaluated as shown in Eq. (4).

The curvature φ of the specimens was obtained from the differential axial strains between the compressive side and the tensile side of the specimens denoted by $A1$ and $A3$, respectively, as shown in Fig. 9. The axial strains were measured from Pi-gauges located at the mid-height of the columns, and were used to calculate the curvature of the columns as follows:

$$\phi = \frac{\varepsilon_{A1} - \varepsilon_{A3}}{D} \quad (5)$$

where ε_{A1} and ε_{A3} are the longitudinal strains at the compression face and tension face of the column, respectively; and D is the diameter of the column.

The results presented in Fig. 12 clearly show the CFRP-confinement and the SMA-confinement of the RC columns increased the moment capacity and the curvature capacity, when compared to the unconfined RC columns under varying eccentric loading. As discussed earlier, the hoop confinement benefits of the CFRP sheets and the SMA wires were minimal at high load eccentricities because the columns response is dominated by flexure resulting in negligible increases in the moment capacity and curvature capacity of the column.

The results in Fig. 12 also indicate actively confining the RC columns with SMA wires significantly enhanced the bending stiffness, moment capacity and curvature capacity compared to the conventionally CFRP-confined columns. This ensures that the active confinement provided by the SMA spirals exhibited an effective role in controlling the crack opening and propagation allowing the column to deform significantly prior to failure.

6.7. Lateral deformation

The lateral displacements recorded along the height of the unconfined, CFRP-confined, and SMA-confined RC columns is presented in Fig. 13. The lateral deformations are compared at loads corresponding to the unconfined column strength, and at the maximum and ultimate capacity of the tested columns. The measured lateral deflections of the columns shown in Fig. 13 were induced due to initial load eccentricity and second order moments.

The results clearly demonstrate the lateral deformation capacity corresponding to maximum loads of the CFRP-confined and SMA-confined RC columns were improved, when compared to the unconfined columns subjected to varying load eccentricities. This behaviour is expected since the additional confinement provided by the externally confined CFRP sheets and SMA wires delayed the local buckling of the internal steel increasing the flexural deformations of the columns. The results also show the enhancement in the flexural capacity was more pronounced for the SMA-confined RC columns when compared to the CFRP-confined RC columns at ultimate loads. The SMA-confined RC columns displayed long and stable post peak responses causing significant increases in the axial deformability of the column that allowed for higher flexural deformations. The improvement in the lateral deformability of the SMA-confined RC columns is attributed to the effectiveness of the active confinement pressure applied by the SMA wires to control the development and propagation of the cracks until the failure point.

The benefits of active confinement can be further established by comparing the lateral deflections of the tested columns at loads corresponding to the unconfined column strength. It is apparent in Fig. 13 the confinement mechanism through active SMA wires and passive CFRP sheets increased the initial axial stiffness of the column, which in turn reduced the measured lateral deformations of the columns when compared to the unconfined RC columns. The results also show RC columns confined with SMA wires experienced higher axial stiffness reflected by the minimal lateral deformations recorded compared to the conventional CFRP-confined and the unconfined RC columns. The passive confinement of the RC columns experienced enhancements in the axial stiffness of the columns only when the CFRP sheets became activated at loads approaching the unconfined column strength. The active confinement mechanism allowed the SMA wires to engage during the early stages of loading and resist the lateral expansion of the concrete that resulted in increasing the initial axial stiffness of the column. The active confinement mechanism was also effective in achieving stiffer lateral deformation response at maximum loads for the SMA-confined RC columns, compared to the passively CFRP-confined columns and the unconfined columns.

As discussed earlier, the hoop confinement of the columns with CFRP sheets and SMA wires had negligible effects on the lateral deformation capacity compared to the unconfined RC columns at high load eccentricities. The reason is because the hoop confinement is ineffective for flexurally-dominated behaviour experienced by columns subjected to high load eccentricities.

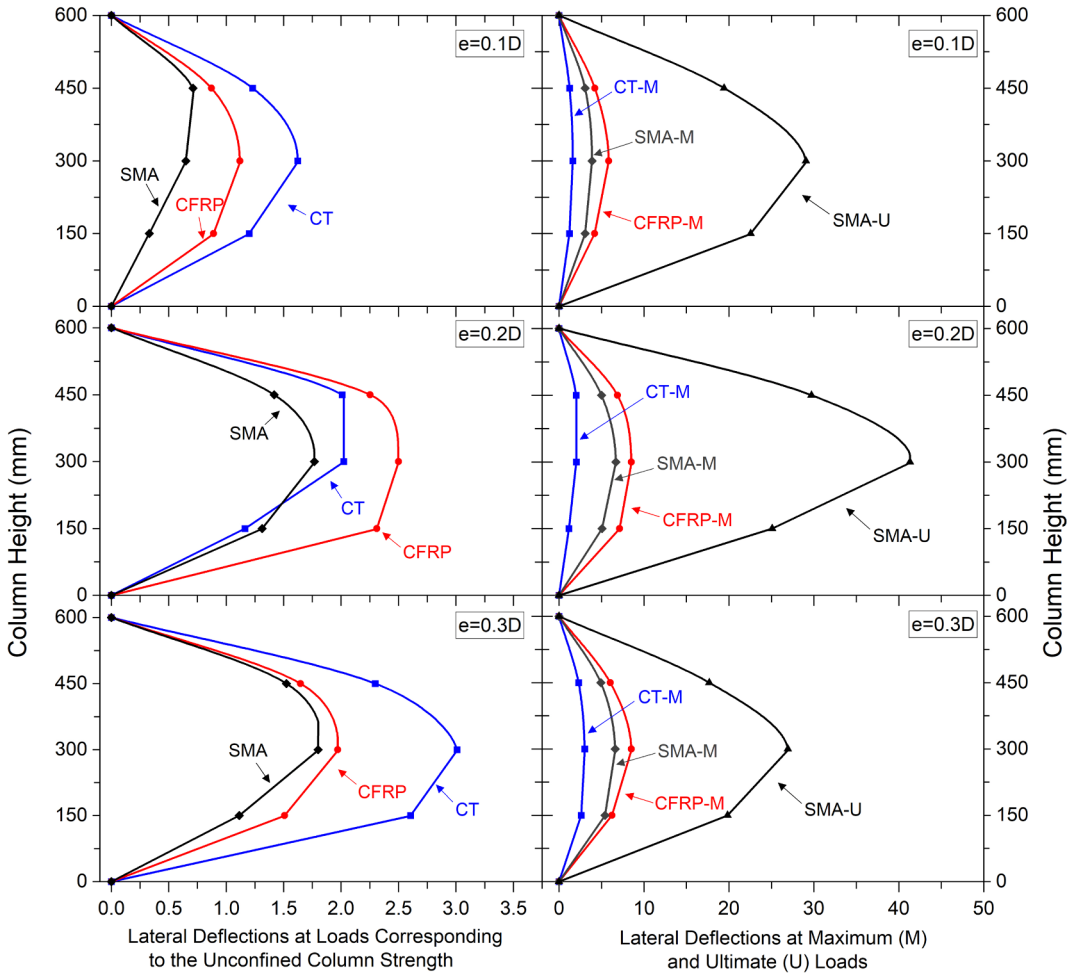

Fig. 13. Lateral deflection response of unconfined RC columns, CFRP-confined RC columns and SMA-confined RC columns.

6.8. Ductility

The effect of using passive CFRP-confinement and active SMA-confinement on the ductility of the concrete columns was examined. Ductility is defined as the ability of the member to absorb inelastic energy without losing its load capacity [50]. For comparison purposes, a ductility index (κ) was defined as a measure of ductility calculated as the area under the axial load-deflection curve up to 20% drop of the ultimate capacity of the column in the descending portion of the curve (Fig. 14).

The results presented in Fig. 14 displays the ductility index κ (normalized to the unconfined concentric case) versus initial axial load eccentricity. The results clearly indicate that the confinement of columns with CFRP sheets and SMA wires significantly enhanced the ductility of the confined columns, when compared to the unconfined columns subject to varying load eccentricity. The maximum ductility benefits were realized in the concentric loaded columns and this was expected because the confinement jacket (CFRP sheet/SMA wires) was activated along the entire circumference of the columns. The relation between the ductility index (κ) and the initial load eccentricity was found to behave in a polynomial manner. The results show that applying a load eccentricity as small as 0.1*D* (15 mm) can cause a significant reduction in the ductility capacity of the columns. A slight reduction in the ductility capacity of the column was observed as the applied load eccentricity increased from 0.1*D* (15 mm) to 0.3*D* (45 mm).

It is also apparent from Fig. 14 the ductility performance of the RC columns confined with the SMA spirals improved significantly. The

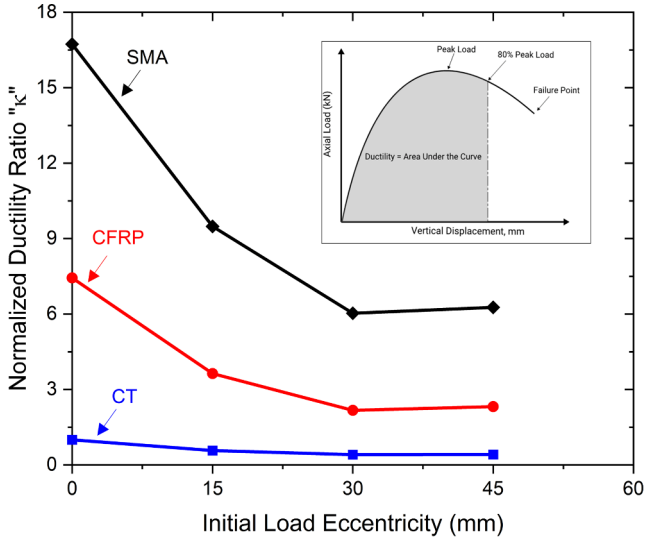

Fig. 14. Normalized ductility index "κ" vs. initial load eccentricity.

ductility index (κ) of the SMA-confined RC columns increased by up to 1.7 times and 9 times compared to the conventional CFRP-confined RC columns and the unconfined RC columns, respectively. The superiority in the ductility performance of the SMA-confined RC columns is attributed to the active confinement pressure applied by the SMA spirals that effectively controlled the development and propagation of the

cracks causing the concrete columns to exhibit smooth and gradual softening of the load-displacement response at the post-peak phase.

7. Conclusions and summary

This experimental study focused on investigating the performance of actively SMA-confined RC columns subjected to eccentric loading, and compare its behaviour to the conventional CFRP-confined RC columns and unconfined RC columns. Based on the results presented herein, the following conclusions can be drawn:

1. Actively confining the RC columns with SMA spirals increased significantly the strength and deformability compared to identical unconfined RC columns subjected to varying eccentric loading. The attained strength capacity of the CFRP-confined and the SMA-confined RC columns were similar as the axial stiffness of both systems were comparable. However, the deformation capacity of the SMA-confined RC columns was increased significantly compared to the conventional CFRP-confined RC columns;
2. The reductions in the strength capacity of the CFRP-confined and SMA-confined columns was more pronounced than the unconfined columns, with the increase in the eccentric distance of the applied load. At minimum load eccentricity, the strength reductions predicted by the CSA A23.3-14 was conservative in the case of the unconfined RC columns and slightly unconservative in the case of the CFRP-confined and SMA-confined RC columns;
3. The initial axial stiffness of the SMA-confined RC columns was increased due to the engagement of the actively confined SMA wires during the initial stages of loading, in comparison to the passively CFRP confined RC columns that experienced enhancements in the axial stiffness of the columns only when the CFRP sheets become activated at loads approaching the unconfined column strength;

In summary, the SMA-confined RC columns demonstrated superior overall performance compared to the conventional CFRP-confined RC columns. The main reason is attributed to the ductile response of the SMA spirals and the active confinement provided by the SMA spirals that exhibited an effective role in controlling and crack opening and propagation allowing the column to deform significantly prior to failure. Further experimental research is critically needed to understand the effects of column size, steel reinforcement ratio's, and concrete compressive strengths on the behaviour of SMA-confined RC columns. Furthermore, research is needed to develop strength and strain prediction equations for SMA-confined RC columns to be implemented by designers for industrial applications.

Acknowledgments

The authors would like to express their gratitude to the University of Calgary and NSERC for the financial support to this research project. The authors are also grateful to Sika Canada for providing the CFRP sheets and the epoxy.

References

[1] Mirza S, Ali M.S. Canada's infrastructure crisis: where do we go from here? In: Proceedings of the seventh international conference on FRP composites in civil engineering (CSCE 2014). Vancouver, Canada; 2014: p. 6.
[2] Mortazavi A, Pilakoutas K, Son KSRC. column strengthening by lateral pre-tensioning of FRP. Constr Build Mater 2002;17(6–7):491–7.
[3] Yan Z, Pantelides C.P, Reaveley L.D. Seismic retrofit of bridge columns using fiber reinforced polymer composite shells and shape modification. In: Proceedings of the fourteen world conference on earthquake engineering. Beijing, China; 2008: p. 8.
[4] Reisi M, Mostofinejad D, Azizi N. M-P curves for strengthened concrete columns with active confinement. In: Proceedings of the fourteen world conference on earthquake engineering. Beijing, China; 2008: p. 8.
[5] Janke L, Czaderski C, Motavalli M, Ruth J. Applications of shape memory in civil engineering structures – overview, limits and new ideas. Mater Struct 2005;38(5):578–92.
[6] Abdelrahman K, El-Hacha R. Preliminary experimental investigation of SMA confined concrete. In: Proceedings of the international conference on concrete repair, rehabilitation and retrofitting (ICCRRR). Leipzig, Germany; 2015: p. 8.
[7] Choi E, Nam T-H, Yoon S-J, Cho S-K, Park J. The behavior of concrete cylinders confined by shape memory alloy wires. Smart Mater Struct 2008;17(6):10.
[8] Andrawes B, Shin M, Wierschem N. Active confinement of reinforced concrete bridges using shape memory alloys. J Bridge Eng ASCE 2010;15(1):81–9.
[9] Shin M, Andrawes B. Experimental investigation of actively confined concrete using shape memory alloys. Eng Struct 2010;32(3):656–64.
[10] Karbhari V, Yanqiang G. Composite jacketed concrete under uniaxial compression – Verification of simple equations. J Mater Civ Eng ASCE 1997;9(4):185–93.
[11] Shahawy M, Mirmiran A. Behavior of concrete columns confined by fiber composites. J Struct Eng ASCE 1997;123(5):583–90.
[12] Mirmiran A, Shahawy M, Samaan M, Echary HE, Mastrapa JC, Pico O. Effect of column parameters on FRP-confined concrete. J Compos Constr ASCE 1998;2(4):175–85.
[13] Toutanji H. Stress-strain characteristics of concrete columns externally confined with advanced fiber composite sheets. ACI Mater J 1999;96(1):391–404.
[14] Shahawy M, Mirmiran A, Beitelman T. Tests and modeling of carbon-wrapped concrete columns. Compos B 2000;31(6–7):471–80.
[15] Sheikh SA. Performance of concrete structures retrofitted with fiber reinforced polymers. Eng Struct 2002;24(7):869–79.
[16] Lam L, Teng JG. Design-oriented stress-strain model for FRP-confined concrete. Constr Build Mater 2003;17(6):471–89.
[17] Mattys S, Toutanji H, Taerwe L. Stress-strain behaviour of large-scale circular columns confined with FRP composites. J Struct Eng ASCE 2006;132(1):123–33.
[18] Thermou GE, Pantazopoulou SJ. Metallic fabric jackets: an innovative method for seismic retrofitting of substandard RC prismatic members. Struct Concr J, fib J, Thomas Telford 2007;8(1):35–46.
[19] Abdelrahman K, El-Hacha R. Behavior of large-scale concrete columns wrapped with CFRP and SFRP sheets. J Compos Constr ASCE 2012;16(4):430–9.
[20] El-Hacha R, Mashrik MA. Effect of SFRP confinement on circular and square concrete columns. Elsevier J Eng Struct 2012;36(10):379–93.
[21] El-Hacha R, Abdelrahman K. Slenderness effect of circular concrete specimens confined with SFRP sheets. Compos B 2013;44(1):152–66.
[22] Abdelrahman K, El-Hacha R. Finite element modeling of concrete columns wrapped with CFRP and SFRP sheets. In: Proceedings of the eight international conference on analytical models and new concepts in concrete and masonry structures (AMCM 2014). Wroclaw, Poland; 2014: p. 8.
[23] Abdelrahman K, El-Hacha R. State-of-the-art review on FRP strengthened concrete columns. In: Proceedings of the international conference on concrete solutions. Queen's University, Belfast, UK; 2014: p. 6.
[24] Chaallal O, Shahawy M. Performance of fiber-reinforced polymer-wrapped reinforced concrete column under combined axial-flexural loading. ACI Struct J 2000;97(4):659–88.
[25] Parvin A, Wang W. Behaviour of FRP jacked concrete columns under eccentric loading. J Compos Constr ASCE 2001;5(3):146–52.
[26] Fam A, Flisak B, Rizkalla S. Experimental and analytical modeling of concrete-filled fiber-reinforced polymer tubes subjected to combined bending and axial loads. ACI Struct J 2003;100(4):499–509.
[27] Hadi MNS. Behaviour of FRP wrapped normal strength concrete columns under eccentric loading. Compos Struct 2006;72(4):503–11.
[28] Hadi MNS. Behaviour of FRP strengthened concrete columns under eccentric compression loading. Compos Struct 2007;77(1):92–6.
[29] Bisby L, Ranger M. Axial-flexural interaction in circular FRP-confined reinforced concrete columns. Constr Build Mater 2010;24(9):1672–81.
[30] Fitzwilliam J, Bisby L. Slenderness effects on circular CFRP confined reinforced concrete columns. J Compos Constr ASCE 2010;14(3):280–8.
[31] Sadeghian P, Rahai AR, Ehsani MR. Experimental study of rectangular RC columns strengthened with CFRP composites under eccentric loading. J Compos Constr ASCE 2010;14(4):443–50.
[32] Krustulovic-Opara N, Thiedmeman PD. Active confinement of concrete members with self-stressing composites. ACI Mater J 2000;93(3):297–308.
[33] Choi E, Nam T-H, Yoon S-J, Cho S-K, Park J. Confining jackets for concrete cylinder using NiTiNb and NiTi shape memory alloys wires. Physica Scripta T 2010;139:4.
[34] Destrebecq J-F, Balandraud X. Interaction between concrete cylinders and shape memory wires in the achievement of active confinement. Mater Complex Behav, Adv Struct Mater 2010;6:19–34.
[35] Mirzaee Z, Moavalli M, Shekarchi M. Experimental investigation of compressive concrete elements confined with shape memory Ni-Ti wires. In: Proceedings of the fracture mechanics of concrete elements and concrete structures – assessment, durability, monitoring and retrofitting of concrete structures. Korea Concrete Institute, Seoul; 2010: p. 1173–78.
[36] Zuboski G.R. Stress-strain behaviour for actively confined concrete using shape memory alloys [MSc Thesis]. USA: The Ohio State University; 2013: p. 213.
[37] Tran H, Balandraud X, Destrebecq JF. Improvement of the mechanical performance of concrete cylinders confined actively or passively by means of SMA wires. Elsevier Urban Partner 2014;8:pp.
[38] Buehler WJ, Gilfrich JV, Wiley RC. Effects of low-temperature phase changes on the mechanical properties of alloys near composition TiNi. J Appl Phys 1963;34(5):3232–9.
[39] Alam MS, Youssef MA, Nehdi M. Utilizing shape memory alloys to enhance the performance and safety of civil infrastructure: a review. Can J Civ Eng 2007;34(34):1075–86.
[40] Sika, Sikawrap® Hex 230C. Product technical data sheet, retrieved Feb. 21, 2010 from http://www.sikaconstruction.com/tds-cpd-SikaWrapHex230C-us.pdf.

[41] Sikadur, Sikadur® 330. Product technical data sheet, retrieved Feb. 21, 2010 from http:/ca01.webdms.sika.com/fileshow.do?documentID=111.
[42] ASTM International. Standard test method of compressive strength of cylindrical concrete specimens. ASTM C39/C39M-17, V. 4.02. West Conshohocken, PA, USA: American Society for Testing Material; 2017.
[43] ASTM International. Standard test methods and definitions for mechanical testing of steel products. ASTM A370-17, V. 01.03. West Conshohocken, PA, USA: American Society for Testing Material; 2017.
[44] ASTM International. Standard test method for tensile properties of polymer matrix composite materials. ASTM D3039/D3039M-14, V. D30.04. West Conshohocken, PA, USA: American Society for Testing Material; 2017.
[45] Memry. SEAS Group Company, http://www.memry.com/products-services/material/wire, retrieved on 15 January 2015.
[46] Abdelrahman K. Performance of eccentrically loaded reinforced concrete columns confined with Shape Memory Alloy wires [Ph.D thesis]. Calgary, Canada: Department of Civil Engineering, University of Calgary; 2017: p. 473.
[47] MacGregor JG, Bartlett MF. Reinforced concrete: mechanics and design. Canada: Prentice-Hall; 2000.
[48] Canadian Standard Associations CSA. Design of concrete structures. A23.3-04, Ontario, Canada; 2004.
[49] Canadian Standard Associations CSA. Design of concrete structures. A23.3-14, Ontario, Canada; 2014.
[50] Issa MA, Alrousan RZ, Issa MA. Experimental and parametric study of circular short columns confined with CFRP composites. J Compos Constr ASCE 2009;13(2):135–47.